

# Generalized Partial Dynamical Symmetries in Nuclear Spectroscopy

A. Leviatan

*Racah Institute of Physics, The Hebrew University, Jerusalem 91904, Israel*

**Abstract.** Explicit forms of IBM Hamiltonians with a generalized partial dynamical  $O(6)$  symmetry are presented and compared with empirical data in  $^{162}\text{Dy}$ .

A dynamical symmetry corresponds to a situation in which the Hamiltonian is written in terms of the Casimir operators of a chain of nested algebras

$$G_1 \supset G_2 \supset \dots \supset G_n , \quad (1)$$

and has the following properties. (i) Solvability. (ii) Quantum numbers related to irreducible representations (irreps) of the algebras in the chain. (iii) Symmetry-dictated structure of wave functions independent of the Hamiltonian's parameters. The merits of a dynamical symmetry are self-evident, however, in most applications to realistic systems, one is compelled to break it. Partial dynamical symmetry (PDS) corresponds to a particular symmetry breaking for which some (but not all) of the above virtues of a dynamical symmetry are retained. Two types of partial symmetries were encountered so far. The first type correspond to a situation for which **part** of the states preserve **all** the dynamical symmetry. This is the case for the  $SU(3)$  PDS found in the IBM-1 [1, 2] and the Symplectic Shell Model [3, 4], and for the  $F$ -spin PDS in the IBM-2 [5]. The corresponding PDS Hamiltonians have a subset of solvable states with good symmetry while other eigenstates are mixed. A second type of partial symmetries correspond to a situation for which **all** the states preserve **part** of the dynamical symmetry. This occurs, for example, when the Hamiltonian preserves only some of the symmetries  $G_i$  in the chain (1) and only their irreps are unmixed [6, 7]. In this case there are no analytic solutions, yet selected quantum numbers (of the conserved symmetries) are retained. In the present contribution we show that it is possible to combine both types of partial symmetries, namely, to construct a Hamiltonian for which **part** of the states have **part** of the dynamical symmetry. We refer to such a structure as a generalized partial dynamical symmetry [8].

Partial symmetry of the second kind was recently considered in [7] in relation to the chain

$$U(6) \supset O(6) \supset O(5) \supset O(3) . \quad (2)$$

The Hamiltonian employed has two- and three-body interactions of the form

$$H_1 = \kappa_0 P_0^\dagger P_0 + \kappa_2 \left( \Pi^{(2)} \times \Pi^{(2)} \right)^{(2)} \cdot \Pi^{(2)} . \quad (3)$$

The  $\kappa_0$  term is the  $O(6)$  pairing term defined in terms of monopole ( $s$ ) and quadrupole ( $d$ ) bosons,  $P_0^\dagger = d^\dagger \cdot d^\dagger - (s^\dagger)^2$ . It is diagonal in the dynamical symmetry basis  $[[N], \sigma, \tau, L]$  of Eq. (2) with eigenvalues  $\kappa_0(N - \sigma)(N + \sigma + 4)$ . The  $\kappa_2$  term is composed only of the  $O(6)$  generator:  $\Pi^{(2)} = d^\dagger s + s^\dagger \tilde{d}$ , which is not a generator of  $O(5)$ . Consequently,  $H_1$  cannot connect different  $O(6)$  irreps but can induce  $O(5)$  mixing. The eigenstates have good  $\sigma$  but not good  $\tau$  quantum numbers.

To consider a generalized  $O(6)$  PDS, we introduce the following IBM-1 Hamiltonian,

$$H_2 = h_0 P_0^\dagger P_0 + h_2 P_2^\dagger \cdot \tilde{P}_2. \quad (4)$$

The  $h_0$  term is identical to the  $\kappa_0$  term of Eq. (3), and the  $h_2$  term is defined in terms of the boson pair  $P_{2,\mu}^\dagger = \sqrt{2}s^\dagger d_\mu^\dagger + \sqrt{7}(d^\dagger d^\dagger)_\mu^{(2)}$  with  $\tilde{P}_{2,\mu} = (-)^\mu P_{2,-\mu}$ . The latter term can induce both  $O(6)$  and  $O(5)$  mixing. Although  $H_2$  is not an  $O(6)$  scalar, it has an exactly solvable ground band with good  $O(6)$  symmetry. This arises from the fact that the  $O(6)$  intrinsic state for the ground band

$$|c; N\rangle = (N!)^{-1/2} (b_c^\dagger)^N |0\rangle, \quad b_c^\dagger = (d_0^\dagger + s^\dagger)/\sqrt{2}, \quad (5)$$

has  $\sigma = N$  and is an exact zero energy eigenstate of  $H_2$ . Since  $H_2$  is rotational invariant, states of good angular momentum  $L$  projected from  $|c; N\rangle$  are also zero-energy eigenstates of  $H_2$  with good  $O(6)$  symmetry, and form the ground band of  $H_2$ . It follows that  $H_2$  has a subset of solvable states with good  $O(6)$  symmetry ( $\sigma = N$ ), which is not preserved by other states. All eigenstates of  $H_2$  break the  $O(5)$  symmetry but preserve the  $O(3)$  symmetry. These are precisely the required features of a generalized partial dynamical symmetry as defined above for the chain of Eq. (2).

In Fig. 1 we show the experimental spectrum of  $^{162}\text{Dy}$  and compare with the calculated spectra of  $H_1$  and  $H_2$ . The spectra display rotational bands of an axially-deformed nucleus, in particular, a ground band ( $K = 0_1$ ) and excited  $K = 2_1$  and  $K = 0_2$  bands. An  $L \cdot L$  term was added to both Hamiltonians, which contributes to the rotational splitting but has no effect on wave functions. The parameters were chosen to reproduce the excitation energies of the  $2_{K=0_1}^+$ ,  $2_{K=2_1}^+$  and  $0_{K=0_2}^+$  levels. The  $O(6)$  decomposition of selected bands is shown in Fig. 2. For  $H_2$ , the solvable  $K = 0_1$  ground band has  $\sigma = N$  and exhibits an exact  $L(L+1)$  splitting. The  $K = 2_1$  band is almost pure with only 0.15% admixture of  $\sigma = N - 2$  into the dominant  $\sigma = N$  component. The  $K = 0_2$  band has components with  $\sigma = N$  (85.50%),  $\sigma = N - 2$  (14.45%), and  $\sigma = N - 4$  (0.05%). Higher bands exhibit stronger mixing, *e.g.*, the  $K = 2_3$  band shown in Fig. 2, has components with  $\sigma = N$  (50.36%),  $\sigma = N - 2$  (49.25%),  $\sigma = N - 4$  (0.38%), and  $\sigma = N - 6$  (0.01%). The  $O(6)$  mixing in excited bands of  $H_2$  depends critically on the ratio  $h_2/h_0$  in Eq. (4) or equivalently on the ratio of the  $K = 0_2$  and  $K = 2_1$  bandhead energies. In contrast, all bands of  $H_1$  are pure with respect to  $O(6)$ . Specifically, the  $K = 0_1, 2_1, 2_3$  bands shown in Fig. 2 have  $\sigma = N$  and the  $K = 0_2$  band has  $\sigma = N - 2$ . In this case the diagonal  $\kappa_0$  term in Eq. (3) simply shifts each band as a whole in accord with its  $\sigma$  assignment. All eigenstates of both  $H_1$  and  $H_2$  are mixed with respect to  $O(5)$ .

To gain more insight into the underlying band structure of  $H_2$  we perform a band-mixing calculation by taking its matrix elements between large- $N$  intrinsic states. The

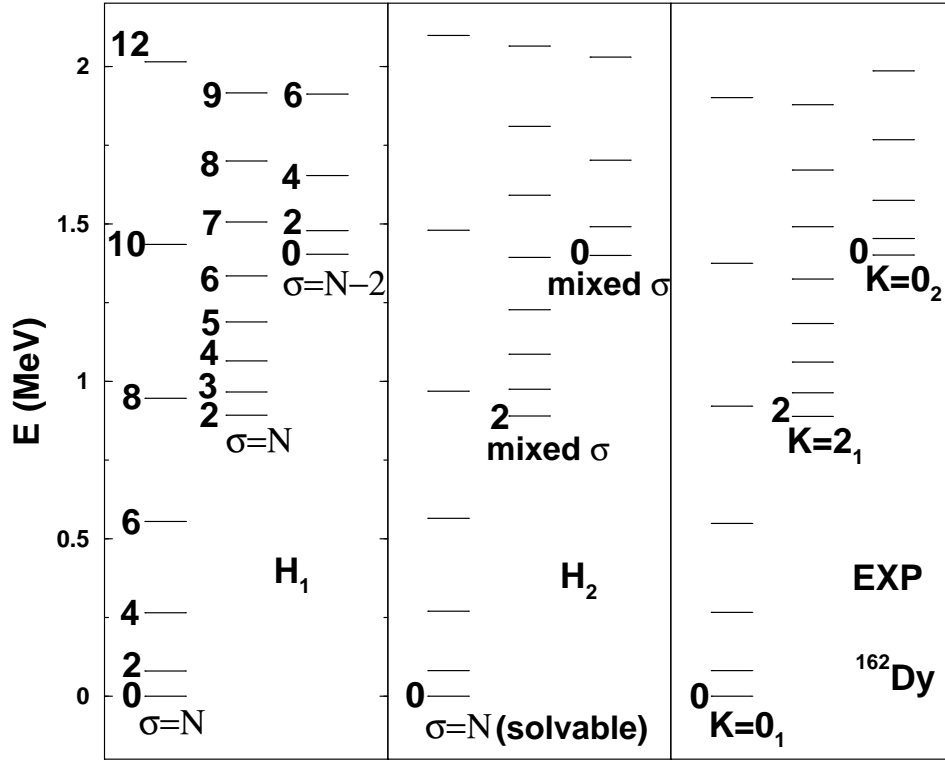


**FIGURE 1.** Experimental spectra (EXP) of  $^{162}\text{Dy}$  [9,10] compared with calculated spectra of  $H_1 + \lambda_1 L \cdot L$ , Eq. (3), and  $H_2 + \lambda_2 L \cdot L$ , Eq. (4), with parameters  $\kappa_0 = 8$ ,  $\kappa_2 = 1.364$ ,  $\lambda_1 = 8$ , and  $h_0 = 28.5$ ,  $h_2 = 6.3$ ,  $\lambda_2 = 13.45$  keV and  $N = 15$ .

latter are obtained in the usual way by replacing a condensate boson in  $|c; N\rangle$  (5) with orthogonal bosons  $b_\beta^\dagger = (d_0^\dagger - s^\dagger)/\sqrt{2}$  and  $d_{\pm 2}^\dagger$  representing  $\beta$  and  $\gamma$  excitations respectively. By construction, the intrinsic state for the ground band of  $H_2$ ,  $|K = 0_1\rangle = |c; N\rangle$ , is decoupled. For the lowest excited bands we find

$$\begin{aligned} |K = 0_2\rangle &= A_\beta |\beta\rangle + A_{\gamma^2} |\gamma_{K=0}^2\rangle + A_{\beta^2} |\beta^2\rangle, \\ |K = 2_1\rangle &= A_\gamma |\gamma\rangle + A_{\beta\gamma} |\beta\gamma\rangle. \end{aligned} \quad (6)$$

Using the parameters of  $H_2$  relevant to  $^{162}\text{Dy}$  (see Fig. 1) we obtain that the  $K = 0_2$  band is composed of 36.29%  $\beta$ , 63.68%  $\gamma_{K=0}^2$  and 0.03%  $\beta^2$  modes, *i.e.*, it is dominantly a double-gamma phonon excitation with significant single- $\beta$  phonon admixture. The  $K = 2_1$  band is composed of 99.85%  $\gamma$  and 0.15%  $\beta\gamma$  modes, *i.e.* it is an almost pure single-gamma phonon band. An  $O(6)$  decomposition of the intrinsic states in Eq. (6) shows that the  $K = 0_2$  intrinsic state has components with  $\sigma = N$  (86.72%),  $\sigma = N - 2$  (13.26%) and  $\sigma = N - 4$  (0.02%). The  $K = 2_1$  intrinsic state has  $\sigma = N$  (99.88%) and  $\sigma = N - 2$  (0.12%). These estimates are in good agreement with the exact results mentioned above in relation to Fig. 2.

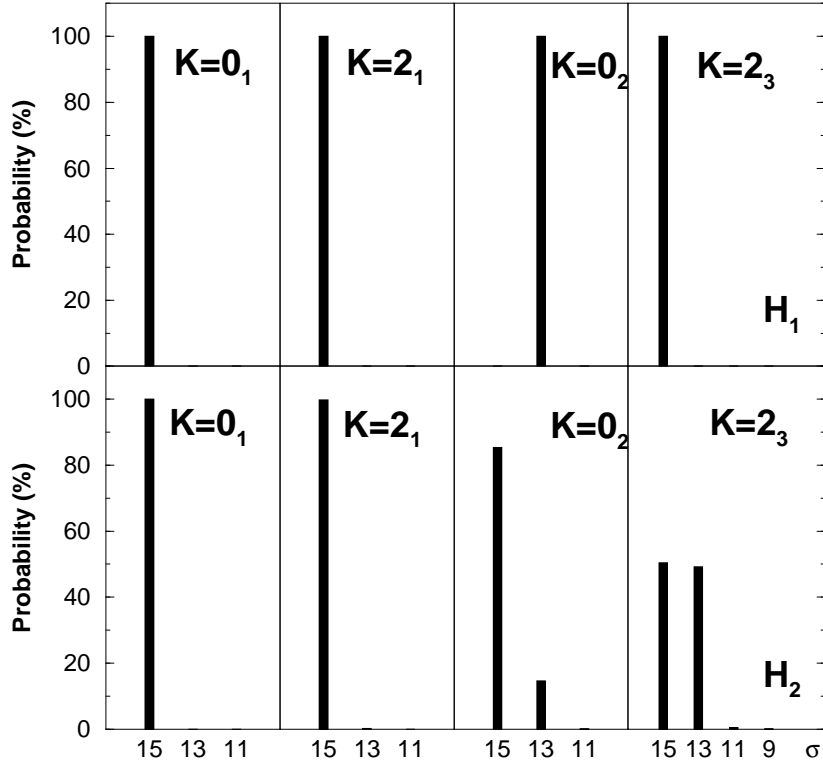


**FIGURE 2.**  $O(6)$  decomposition of wave functions of the  $K = 0_1, 2_1, 0_2, 2_3$  bands for  $H_1$  (upper portion) and  $H_2$  (lower portion).

In Table 1 we compare the presently known experimental  $B(E2)$  values for transitions in  $^{162}\text{Dy}$  with the values predicted by  $H_1$  and  $H_2$  using the  $E2$  operator

$$T^{(2)} = e \left[ \Pi^{(2)} + \chi (d^\dagger \tilde{d})^{(2)} \right]. \quad (7)$$

The parameters  $e$  and  $\chi$  in Eq. (7) were fixed for each Hamiltonian by the empirical  $2_{K=0_1}^+ \rightarrow 0_{K=0_1}^+$  and  $2_{K=2_1}^+ \rightarrow 0_{K=0_1}^+$   $E2$  rates. The  $B(E2)$  values predicted by  $H_1$  and  $H_2$  for  $K = 0_1 \rightarrow K = 0_1$  and  $K = 2_1 \rightarrow K = 0_1$  transitions are very similar and agree well with the measured values. On the other hand, their predictions for interband transitions from the  $K = 0_2$  band are very different. For  $H_1$ , the  $K = 0_2 \rightarrow K = 0_1$  and  $K = 0_2 \rightarrow K = 2_1$  transitions are comparable and weaker than  $K = 2_1 \rightarrow K = 0_1$ . This can be understood if we recall the  $O(6)$  assignments for the bands of  $H_1$ :  $K = 0_1, 2_1$  ( $\sigma = N$ ),  $K = 0_2$  ( $\sigma = N - 2$ ), and the  $E2$  selection rules of  $\Pi^{(2)}$  ( $\Delta\sigma = 0$ ) and  $(d^\dagger \tilde{d})^{(2)}$  ( $\Delta\sigma = 0 \pm 2$ ), which imply that in this case only the  $(d^\dagger \tilde{d})^{(2)}$  term contributes to interband transitions from the  $K = 0_1$  band. In contrast, for  $H_2$ ,  $K = 0_2 \rightarrow K = 2_1$  and  $K = 2_1 \rightarrow K = 0_1$  transitions are comparable and stronger than  $K = 0_2 \rightarrow K = 0_1$ . This behaviour is due to the underlying band structure discussed above, and the fact that  $\langle K = 0_2 | \Pi_0^{(2)} | K = 0_1 \rangle = 0$ , while both terms in Eq. (7) contribute to  $\Delta K = 2$  interband

$E2$  intrinsic matrix elements. Recently the  $B(E2)$  ratios  $R_1 = \frac{B(E2; 0_{K=0_2}^+ \rightarrow 2_{K=2_1}^+)}{B(E2; 0_{K=0_2}^+ \rightarrow 2_{K=0_1}^+)} = 10(5)$

**TABLE 1.** Calculated and observed [10,11]  $B(E2)$  values ( $e^2b^2$ ) for  $^{162}\text{Dy}$ . The  $E2$  parameters in Eq. (7) are  $e = 0.138$  (0.126)  $eb$  and  $\chi = -0.22$  ( $-0.55$ ) for  $H_1$  ( $H_2$ ).

Transition	$H_1$	$H_2$	Expt.	Transition	$H_1$	$H_2$	Expt.
$2_{K=0_1}^+ \rightarrow 0_{K=0_1}^+$	1.06	1.05	1.07(2)	$2_{K=2_1}^+ \rightarrow 0_{K=0_1}^+$	0.024	0.024	0.024(1)
$4_{K=0_1}^+ \rightarrow 2_{K=0_1}^+$	1.50	1.49	1.51(6)	$2_{K=2_1}^+ \rightarrow 2_{K=0_1}^+$	0.038	0.0395	0.042(2)
$6_{K=0_1}^+ \rightarrow 4_{K=0_1}^+$	1.62	1.61	1.57(9)	$2_{K=2_1}^+ \rightarrow 4_{K=0_1}^+$	0.0025	0.0026	0.0030(2)
$8_{K=0_1}^+ \rightarrow 6_{K=0_1}^+$	1.65	1.65	1.82(9)	$3_{K=2_1}^+ \rightarrow 2_{K=0_1}^+$	0.0428	0.0425	
$10_{K=0_1}^+ \rightarrow 8_{K=0_1}^+$	1.63	1.64	1.83(12)	$3_{K=2_1}^+ \rightarrow 4_{K=0_1}^+$	0.022	0.023	
$12_{K=0_1}^+ \rightarrow 10_{K=0_1}^+$	1.58	1.60	1.68(21)	$4_{K=2_1}^+ \rightarrow 2_{K=0_1}^+$	0.0123	0.0114	0.0091(5)
				$4_{K=2_1}^+ \rightarrow 4_{K=0_1}^+$	0.046	0.047	0.044(3)
$0_{K=0_2}^+ \rightarrow 2_{K=0_1}^+$	0.0014	0.0022		$4_{K=2_1}^+ \rightarrow 6_{K=0_1}^+$	0.0061	0.0061	0.0063(4)
$0_{K=0_2}^+ \rightarrow 2_{K=2_1}^+$	0.0012	0.1707		$5_{K=2_1}^+ \rightarrow 4_{K=0_1}^+$	0.0345	0.033	0.033(2)
$2_{K=0_2}^+ \rightarrow 0_{K=0_1}^+$	0.0002	0.0004		$5_{K=2_1}^+ \rightarrow 6_{K=0_1}^+$	0.029	0.031	0.040(2)
$2_{K=0_2}^+ \rightarrow 2_{K=0_1}^+$	0.0003	0.0005		$6_{K=2_1}^+ \rightarrow 4_{K=0_1}^+$	0.0085	0.0071	0.0063(4)
$2_{K=0_2}^+ \rightarrow 2_{K=2_1}^+$	0.0003	0.0365		$6_{K=2_1}^+ \rightarrow 6_{K=0_1}^+$	0.046	0.047	0.050(4)

and  $R_2 = \frac{B(E2; 2_{K=0_2}^+ \rightarrow 4_{K=0_1}^+)}{B(E2; 2_{K=0_2}^+ \rightarrow 0_{K=0_1}^+)} = 65(28)$  have been measured [9]. The corresponding predictions are  $R_1 = 0.86$ ,  $R_2 = 4.00$  for  $H_1$  and  $R_1 = 77.59$ ,  $R_2 = 3.25$  for  $H_2$ . As noted in [9], the empirical value of  $R_2$  deviates ‘beyond reasonable expectations’ from the Alaga rule value  $R_2 = 2.6$ . A measurement of absolute  $B(E2)$  values for these transitions is highly desirable to clarify the origin of these discrepancies.

It is a pleasure to dedicate this article to Rick Casten on the occasion of his 60th birthday, and thank him for many years of illuminating discussions. This work was done in collaboration with P. Van Isacker (GANIL) and was supported in part by the Israel Science Foundation.

## REFERENCES

1. Leviatan, A., *Phys. Rev. Lett.*, **77**, 818 (1996).
2. Leviatan, A., and Sinai, I., *Phys. Rev. C*, **60**, 061301 (1999).
3. Escher, J., and Leviatan, A., *Phys. Rev. Lett.*, **84**, 1866 (2000).
4. Escher, J., and Leviatan, A., *Phys. Rev. C*, **65**, 054309 (2002).
5. Leviatan, A., and Ginocchio, J. N., *Phys. Rev. C*, **61**, 024305 (2000).
6. Talmi, I., *Phys. Lett. B*, **405**, 1 (1997).
7. Van Isacker, P., *Phys. Rev. Lett.*, **83**, 4269 (1999).
8. Leviatan, A., and Van Isacker, P., *Phys. Rev. Lett.*, in press (2002).
9. Zamfir, N. V., *et al.*, *Phys. Rev. C*, **60**, 054319 (1999).
10. Helmer R. G., and Reich, C. W., *Nucl. Data Sheets*, **87**, 317 (1999).
11. Warner, D. D., *et al.*, in *Proc. 6th Conf. on Capture Gamma-Ray Spectroscopy*, edited by K. Abrahams and P. Van Assche, Institute of Physics, Bristol, 1988, p. 562.